Available online at www.sciencedirect.com
SCIENCE DIRECT®

Thermochimica Acta 435 (2005) 188–196

thermochimica acta

www.elsevier.com/locate/tca

Thermal decomposition study of intumescent additives: Pentaerythritol phosphate and its blend with melamine phosphate

A.I. Balabanovich *

Research Institute for Physical Chemical Problems of the Belarusian State University, ul. Leningradskaya 14, 220050 Minsk, Belarus

Received 13 February 2005; received in revised form 8 May 2005; accepted 16 May 2005
Available online 29 June 2005

Abstract

Thermal decomposition of pentaerythritol phosphate (PEPA) and its blend (PEPAMP) with melamine phosphate were studied by TG, DSC, TOF MS, and FTIR of volatile and solid decomposition products. Both PEPA and PEPAMP produce intumescent char on heating, however that of PEPAMP is less stable to thermo-oxidative decomposition. The main decomposition pathway of PEPA is liberation of phosphoric acid followed by formation of a foamed carbonized residue. In the mixture of PEPAMP, reaction between the components occurs, which strongly reduces the heat release peaks of PEPA. In addition, condensates of melamine and their products of hydrolysis are formed. The hydrolysis reaction causes a low-temperature decomposition of the melamine ring, which results in the formation of urea, carbon dioxide and ammonia. The thermal decomposition of PEPA and PEPAMP is discussed.

Keywords: Melamine phosphate; Flame retardance; Pyrolysis; Thermal analysis; FTIR

1. Introduction

Intumescence is a strategy in flame retardancy, which involves the formation on heating of a swollen multicellular thermally stable char insulating the underlying material from the flame action [1]. A typical intumescent system comprises a dehydration catalyst (a) for char formation (usually a phosphoric acid derivative, ammonium polyphosphate for example), a carbon rich polyol compound (b) and an organic amine or amide (c) that are capable of producing the char (a + b) and of blowing it to a foamed structure (+c) [2]. The components can be separately introduced; however, the next developments have been aimed at the synthesis of a single compound, which provides all the functions required for intumescence. One of these compounds is 2,6,7-trioxa-1-phosphabicyclo[2,2,2]octane-4-methanol 1-oxide (pentaerythritol phosphate, PEPA) which has been claimed to be effective as both flame retardant in glass fiber reinforced PET [3], a PPO/HIPS blend [4], epoxy resins [5] and smoke suppressant for thermoset materials [6]. It affects the limiting oxygen index values of poly(butylene terephthalate) (PBT), which steadily increase from 21.9 to 26.9 upon addition of 0–30 wt.% of the additive. Moreover, at the 30 wt.% loading the formation of an intumescent char is observed on the specimens [7].

At the same time, the single component approach might have a drawback because the ratio between the chemical structures performing the different functions is not effective to achieve maximum of the fire retardant effect, and combination with synergistic components may be needed. Thus, compounds of nitrogen are regarded synergistic for PEPA to impart flame retardant and intumescent character to a variety of polymers [8,9]. In PBT, a mixture of PEPA with melamine phosphate (MP) exhibits a stronger effect, as the limiting oxygen index values of the formulations rise from 21.9 to 31.7 upon addition of 0–30 wt.% of the mixture [7]. The synergistic effect is likely to come from reaction between pyrolyzing additives. This study was therefore aimed at elucidation of chemical reactions taking place on pyrolysis of

---

* Tel.: +375 172 224509; fax: +375 172 264696.
E-mail address: balabanovich@bsu.by.

0040-6031/$ – see front matter © 2005 Elsevier B.V. All rights reserved.
doi:10.1016/j.tca.2005.05.019

the mixture of MP and PEPA. For comparison, the thermal decomposition of PEPA was studied as well. In this respect, the pyrolysis studies of another intumescent additive, pentaerythritol diphosphate (3,9-dihydroxy-2,4,8,10-tetraoxa-3,9-diphosphaspiro[5,5]-undecane 3,9-dioxide) [10,11], are of importance for understanding of the thermal decomposition of PEPA.

2. Experimental

2.1. Materials

PEPA(I) Great Lakes NH-1197, registered trademark of Great Lakes Chemical Corporation) and PEPAMP (Great Lakes NH-1511, registered trademark of Great Lakes Chemical Corporation), a blend of PEPA with a phosphate synergist, MP(II), with the overall phosphorus content of about 15% (given by the manufacturer) were used as received.

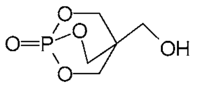

(I)

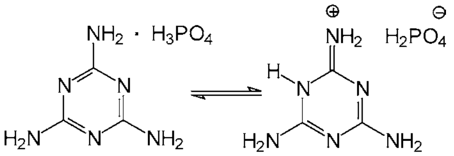

(II)

2.2. Thermal analysis

Thermal analysis was carried out using a Mettler TA 3000 thermal analyzer provided with a thermogravimetry module and a differential scanning calorimetry (DSC) cell. The temperature precision of the thermobalance and of the DSC cell was ±2 and ±0.2 °C correspondingly. The weight data precision was ±1 μg under constant conditions. Standard measurements were performed at a heating rate of 10 °C/min in an argon flow of 90 cm^3/min. The non-volatile fraction reproducibility at 600 °C was ±2%. The sample size was 8–9 mg.

2.3. TOF MS analysis

The experiments were performed on a GCT time-of-flight (TOF) MS detector operating in field ionization (FI) mode, which provides a robust soft ionization MS technique. The detector designed for the characterization of volatile compounds by exact mass measurement.

2.4. Analysis of pyrolysis products

Solid residues collected at different steps of thermal decomposition in thermogravimetry under nitrogen were investigated by IR spectroscopy on a Perkin-Elmer "Spectrum 1000" FTIR spectrometer using KBr pellets.

Moreover, volatile products were collected with the aid of a glass set-up consisting of a round bottom flask (diameter of 3 cm) that contained the sample and of a cold-water condenser at the upper part. While an argon stream passed through, the bottom part was heated up at a rate of 10 °C/min to 400 °C and kept at this temperature for 10 min. High boiling products, HBPs, that condensed at the inner wall of the condenser were collected and analyzed by FTIR. Gaseous products were collected by directing the argon stream from the condenser to a liquid nitrogen trap containing KBr windows and analyzed by FTIR too.

3. Results and discussion

3.1. Thermal analysis

In DSC (Fig. 1), PEPA shows three endothermal phenomena at 115, 145, 167 °C before melting at 218 °C. In addition, two exothermal effects at 296 and 340 °C (Fig. 1) are associated with the two successive steps of weight loss of 17 and 14% in the ranges of 220–310 and 310–360 °C in TG. A 21% weight loss is observed during the third stage at 360–550 °C (Fig. 2). Comparing this thermal behavior (curve 1) to that under air (curve 2) reveals retardation of the weight loss process above 320 °C followed by its acceleration above 440 °C.

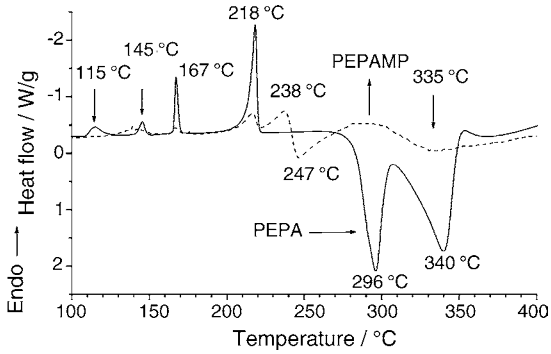

Fig. 1. DSC curves of PEPA and PEPAMP. Run under a nitrogen flow (90 cm^3/min) at a heating rate of 10 °C/min.

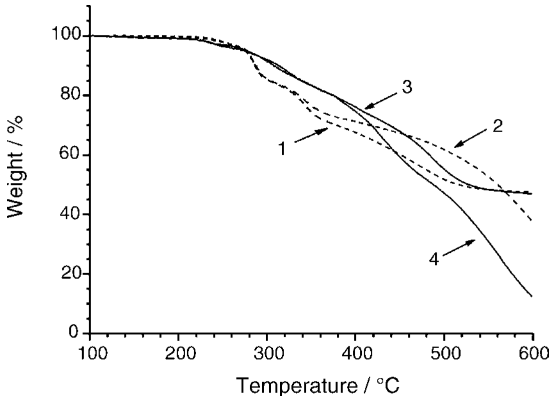

Fig. 2. Thermogravimetry of PEPA (1 and 2) and PEPAMP (3 and 4). Run under a nitrogen (1 and 3) or an air (2 and 4) flow (90 cm^3/min) at a heating rate of 10 °C/min.

As reported in [12,13], MP loses weight very gradually, leaving 33% solid residue at 600 °C. The weight loss at 100–320 °C (6 °C/min) proceeds without melting and is accompanied by two endothermal phenomena at 265 and 305 °C assigned to two dehydratation processes which result in the formation of melamine pyrophosphate and melamine polyphosphate correspondently [13].

The addition of MP changes the thermal decomposition behavior of PEPA remarkably, as the exotherm at 296 °C vanished (Fig. 1). Just after melting of PEPA in PEPAMP, a next endothermal effect is observed followed by an exothermal one. The first effect is attributed to dehydratation of MP (i.e. to the formation of melamine pyrophosphate [14]), whereas the second one can result from reaction between MP and PEPA. It should be noted that the first effect of dehydratation should proceed up to 265 °C [14], indicating that it is interrupted by the exothermal reaction.

In TG, PEPAMP exhibits gradual weight loss leaving 47% solid residue at 600 °C (Fig. 2, curve 3). Thermal oxidation leads to an intensive volatilization of the sample above 380 °C (curve 4).

In conclusion, the data of thermal analysis indicate the occurrence of reaction between PEPA and MP on heating.

3.2. FTIR study of PEPA

When the white powdery PEPA or PEPAMP were subjected to a flame (Fig. 3) or heated in TG, they formed char with intensive foaming (i.e. an intumescent char). Detailed study in TG under nitrogen (10 °C/min) showed that PEPA gave a black solid residue at about 270 °C, which started to form a foamed char at about 280 °C. PEPAMP produced white foam from 270 °C, which started getting “blackness” at about 340 °C. IR spectroscopy has been utilized to study chemical processes occurring in the condensed state of the additives on heating.

Fig. 3. PEPA (50 mg) before (1) and after (2) exposure to flame. PEPAMP (50 mg) before (3) and after (4) exposure to flame.

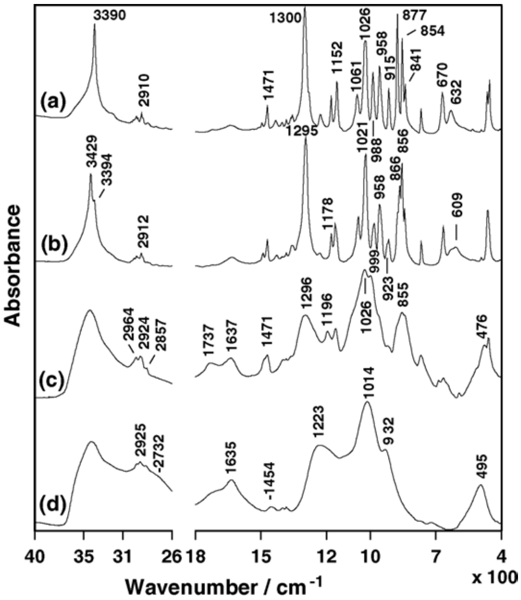

Fig. 4. Infrared spectra of original PEPA (a) and its solid decomposition products collected in thermogravimetry in inert atmosphere on heating (10 °C/min) to: 5% weight loss (b), 20% weight loss (c) and 35% weight loss (d). Pellets in KBr.

The FTIR spectrum of PEPA is shown in Fig. 4 (Spectrum a), band assignments in Table 1. With respect to four absorption bands around 915, 854, 768 and 670 cm^{-1}, they are present in the IR spectra of spirophospates [11,15], bicyclic

Table 1
Assignment of IR absorption bands of PEPA and MP

Band position (cm^{-1})	Assignment	Reference
PEPA		
3390	OH stretch	[21]
2963, 2910	Assymmetric and symmetric CH_2 stretch	[21]
1471	CH_2 deformation	[21]
1300	P=O	[20]
1178, 1152, 1061, 988,455	Not assigned	
1026	Stretching of P–O–C + C–O(H)	[20,21]
958	CH_2OH deformation	Present study
915, 854, 768, 670	Typical of cyclic structures	Present study
877, 841	Typical of bicyclic structures	Present study
632	OH deformation	[21]
Melamine phosphate[a]		
3392, 3158	Assymmetric and symmetric NH stretch	[21]
1673	C=N stretch + NH_2 deformation	[21]
1615, 1557, 1518, 1480, 1407	Ring stretch	[21]
2681, 2341, 1248, 958, 511	Typical of O=P–O–H	[20]
1108, 1050	PO_2^- stretch	[20]
786	Ring deformation	[21]
613	NH_2 deformation	[21]

[a] FTIR absorption bands were taken from a reference melamine phosphate.

phosphites [16,17] and arsenites [17], and bicyclic phosphates [18], i.e. being typical of cyclic structures. Bicyclic phosphites exhibit a strong absorption band around 735 cm^{-1} [17,19]; it moves to 594 cm^{-1} in bicyclic arsenites (replacing phosphorus by arsenic) [17] and to 877 and 841 cm^{-1} in the bicyclic phosphate (Table 1). Therefore, the two latter absorption bands are likely associated with bicyclic $O{=}PO_3$ vibrations. The CH_2–(OH) and OH deformation vibrations absorb at 958 and 632 cm^{-1}. These absorption bands are typical of a bicyclic phosphite $P(OCH_2)_3CCH_2OH$ and arsenite $As(OCH_2)_3CCH_2OH$ and disappear on etherification [17].

At 5% weight loss (Fig. 4, Spectrum b), the OH stretching band at 3390 cm^{-1} decreased in intensity. Simultaneously, a new OH band at 3429 cm^{-1} developed, indicating that there was a production of new alcoholic –OH groups. The same trend was followed by other bands associated with –CH_2–OH and OH groups at 958 and 632 cm^{-1}. In addition, there was a significant decrease of the bicycle-related bands at 877 and 841 cm^{-1}, indicating degradation of the bicyclic structure.

During the first stage of weight loss the –OH band was destroyed (Spectrum c). New bands appeared at 2350 (not shown), 1637, 999 and 476 cm^{-1}, characteristic of a P–OH group [20], whereas a new band at 1737 cm^{-1} is likely attributed to an ester carbonyl [21]. The progression of the P–OH group indicates decomposition of a P–O–C bond. However, the Spectrum (c) is still dominated by strong absorption bands of the P–O–C groups at 1026 cm^{-1}; the 855 cm^{-1} band points to existence of a cyclic structure left undecomposed after the first stage of weight loss.

It is important to note that, during the first stage, the overall profile of the C–H stretch spectral region changed remarkably. The 2912 cm^{-1} band moved to 2924 cm^{-1}. There is an increase in the intensity of the 2964 cm^{-1} band, indicating the formation of new aliphatic bonds [21].

The untouched P–O–C bonds of ring structures vanished during the second stage of weight loss (Spectrum d). The spectrum is dominated by the strong absorption bands of polyphosphoric acids at 2732, 2350 (not shown), 1635, 1223, 1014, 495 cm^{-1} (O=P–OH) and 932 cm^{-1} (P–O–P) [20].

3.3. *Thermal decomposition of PEPA*

Pyrolysis of non-cyclic organophosphorus compounds containing ester P–O–C bond(s) involves elimination reactions to give olefins and corresponding phosphorus-containing acids [22,23]. No carbonaceous residue formation was observed in these reactions. In addition, the pyrolysis studies revealed [22,23] that the thermal stability of the P–O–C bond decreases with increasing branching in the alkyl group in the order ethyl > *n*-octyl ≈ β-phenethyl ≈ *n*-propyl ≈ *s*-butyl > 2-octyl ≈ *i*-Pr > cyclohexyl, as inferred from temperature at which gas evolution starts, i.e. 340, 245, 240, 240, 240, 215, 210 and 195 °C correspondently. A cyclic *cis*-elimination mechanism has been postulated for the thermal decomposition of alkyl esters of phosphorus-containing acids [22].

PEPA starts to decompose after melting (218 °C; Figs. 1 and 2), i.e. at relatively lower temperature although it does not possess any hydrogen atoms on the β-carbon, which are necessary for the cyclic transition state (i.e. for the *cis*-elimination). The reactive alcoholic group and impurities may depress the thermal stability of the P–O–C bonds. The main changes observed in the OH and P–O–C spectral region at 5% weight loss (Fig. 4b) suppose *trans*-esterification of PEPA by the free alcoholic group, which leads to a distraction of the bicycle and production of new alcoholic groups (Fig. 5A, 1st step). In this reaction, three or more molecules can be involved simultaneously.

At the same time with the *trans*-esterification reaction, scission of the P–O–C bond occurs, most likely by carbonium ion mechanism, which has been postulated for the thermal decomposition of pentaerythritol diphosphate [1,11]. In accordance with this mechanism, the formation of carbonium ions occurs from protonation (with an acid impurity or from an acid resulted from hydrolysis of a P–O–C bond, for example) of the phosphoryl group (Fig. 5A, steps 2 and 3) followed by skeleton rearrangement to give the more stable carbonium ion (step 4). In the next step, an olefin is generated by the *cis*-elimination mechanism followed by deprotonation to form a diene. At once, the dienes or olefins formed in this way are involved in exothermal polymerization or Diels–Alder reactions producing new aliphatic bonds (Fig. 4c) and causing the first exotherm in DSC (Fig. 1). Simultaneously, a foamed char is produced.

In the course of the described reactions phosphoric acid moieties are liberated (Fig. 4c). Above 200 °C the P–OH groups quickly condensates to give a pyrophosphate being a strong phosphorylation agent. The phosphorylation of PEPA results in disappearing of the free alcoholic group (Fig. 4c), as shown in Fig. 5B.

At least one P-containing ring is left after the first stage of thermal decomposition at 220–310 °C (Fig. 4c). It undergoes scission on further heating in the range of 310–360 °C by a similar mechanism shown in Fig. 5A, liberating phosphoric acid that condensates to a polyphosphoric acid (Fig. 4d). Olefinic bonds created at this stage are involved in exothermal polymerization again (Fig. 1, the second peak). Aromatization of this residue is likely to occur during this or next step of decomposition.

3.4. *FTIR study of PEPAMP*

The IR spectrum of PEPAMP (Fig. 6, Spectrum a) exhibits the absorption bands of both MP and PEPA (Table 1). By heating to 250 °C there were dramatic spectral changes in all regions of the IR spectrum (Spectrum b). The absorption bands at 1299, 958 and 877 cm^{-1} disappeared, indicating rapid decomposition of PEPA. The sharp 3392 cm^{-1} band due to the OH stretching was eliminated as well. These facts signify reaction of MP and PEPA or of decomposition products of MP and PEPA, as plain PEPA keeps certain absorption bands (P=O, P–O–C) up to 300 °C (Fig. 4,

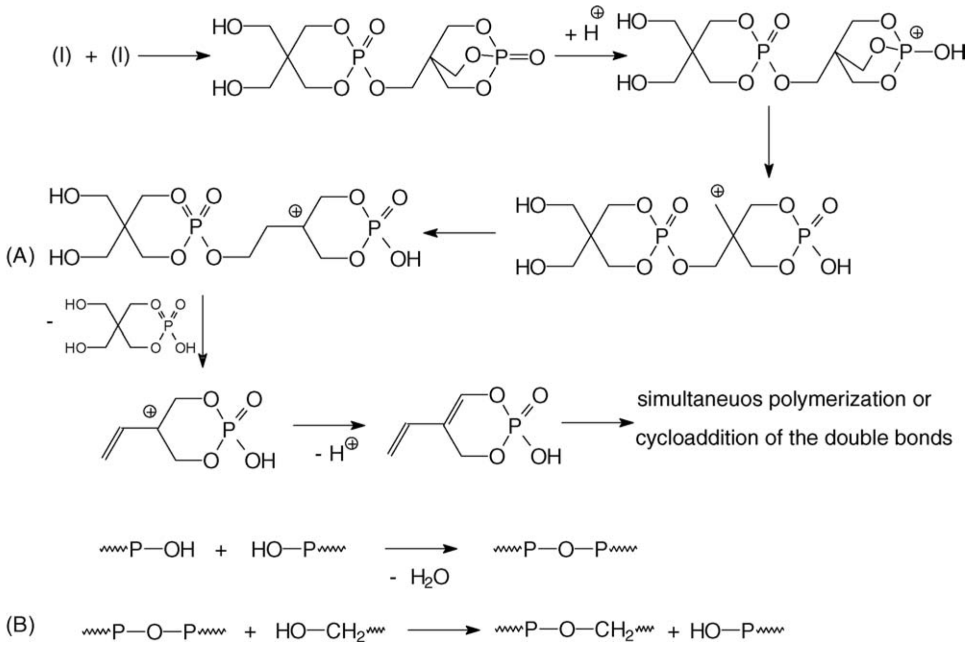

Fig. 5. Proposed mechanism of the formation of phosphoric acid moieties during the first stage of the pyrolysis of PEPA (A) and of the phosphorylation of PEPA (B).

Spectrum b). The additional support for the reaction comes from the exothermic effect at 247 °C in DSC (Fig. 1), as neither PEPA nor MP [14] exhibit an exothermic effect at this temperature.

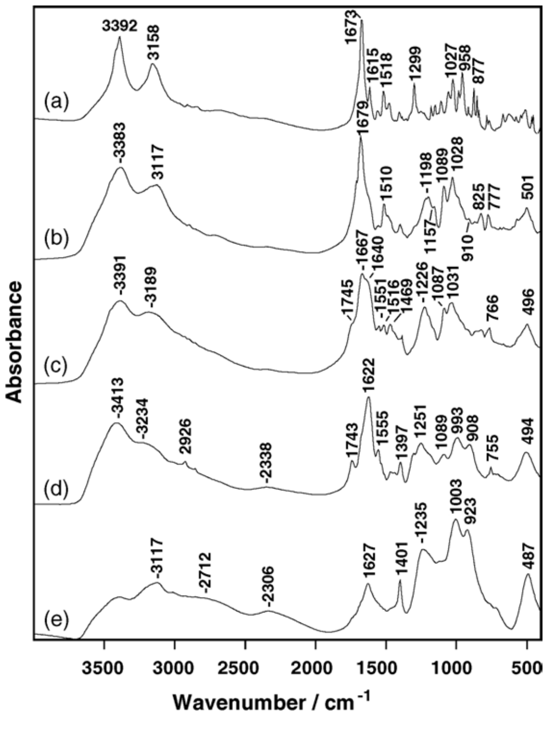

Fig. 6. Infrared spectra of original PEPAMP (a) and its solid products of the thermal decomposition collected in thermogravimetry in inert atmosphere on heating (10 °C/min) to 250 °C (b), 300 °C (c), 400 °C (d) and 500 °C (e). Pellets in KBr.

New absorption bands at 1198 and 1157 cm^{-1} appeared in Spectrum b, associated with the formation of a pyrophosphate salt. The bands were assigned based on the IR spectrum of a reference melamine pyrophosphate. This result is in agreement with the data on the pyrolysis of MP [13]; the pyrophosphate anion undergoes decomposition at 300–330 °C [13].

However, in contrast to the pyrolysis of MP, the formation of the pyrophosphate is not a dominant process at 250 °C. Formation of another product was revealed from the appearance of bands at 1225 (shoulder), 1089, 1028 and 501 cm^{-1}, ascribable to a phosphate or monobasic phosphate anion [24] (see also Fig. 7, Spectrum d). The product was dominant at 300 °C (Spectrum c) and mostly destroyed at 400 °C (Spectrum d), probably with liberation of polyphosphoric acids, as detected by their absorption bands at 2338, 1251 (broad), 993, 908 and 496 cm^{-1}.

A next set of reactions is generated by amino groups, started between 250 and 300 °C, as inferred from the development of a strong shoulder at 1640 cm^{-1} at 300 °C (Spectrum c), ascribable to the deformation vibration of a primary and/or of a protonated secondary amino group. By further heating to 400 °C the 1673 cm^{-1} band was eliminated (Spectrum d), and the shoulder at 1640 cm^{-1} moved and ended up at 1622 cm^{-1} being one of the major and strongest peaks in the Spectrum (d), associated with the formation of a protonated tertiary amino group [25]. It persisted heating to 500 °C (Spectrum e). One of possible reactions causing these transformations is a progressive condensation of the primary amino groups to the secondary and tertiary ones.

A next product not observed in the pyrolysis study of MP [13] is associated with the shoulder at 1745 cm^{-1} ascribable

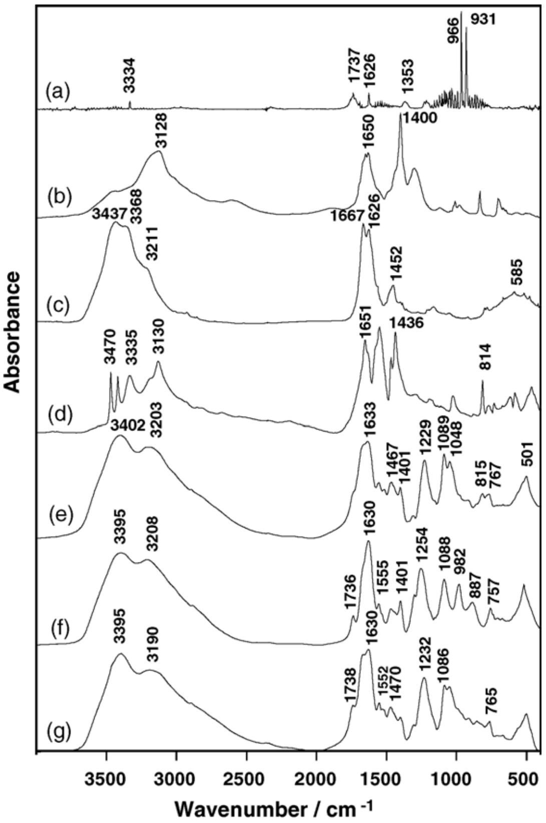

Fig. 7. FTIR spectra of the gaseous (a) and condensable (b–g) pyrolysis products of PEPAMP emitted in the degradation apparatus.

to a C═O stretch. The shoulder formed at 300 °C (Spectrum c) and transformed to a real peak at 400 °C (Spectrum d; see also Fig. 7, Spectrum f) disappearing on further heating to 500 °C (Spectrum e). It is plausible supposing that the absorption band develops from transformations of melamine and is indicative of ammeline-type (4,6-diamino-1,3,5-triazin-2(1H)-one) structures [26] (hydrolysis of melamine).

At 500 °C, the polyphosphoric acid moieties became dominant in the residue (Spectrum e). The absorption bands at 3117 and 1401 cm^{-1} are characteristic of ammonium [21]. These bands were observed in the pyrolysis residue of PBT fire retarded with ammonium polyphosphate and 2-methyl-1,2-oxaphospholan-5-one 2-oxide [27]. Weil et al. [28] found the similar absorption bands in the IR spectrum of the pyrolysis residue of EVA fire retarded with 5,5,5′,5′,5″,5″-hexamethyltris(1,3,2-dioxaphosphorinanemethan)amine 2,2′,2″-trioxide and melamine pyrophosphate and assigned them to an artifact from hydrolysis of some of the imidophosphoric acid subsequent to the char formation.

The main gaseous pyrolysis product of PEPAMP is ammonia (Fig. 7, spectrum a) [26]. Some volatile carbonyl compounds are formed in a much lower yield, as detected by the absorption band at 1737 cm^{-1} [21]. The next minor gaseous product is carbon dioxide. It undergoes reaction with ammonia, producing ammonium carbamate that forms white crystals at the wall in the upper part of the condenser. Its FTIR spectrum (Fig. 7, Spectrum b) is identical to that of a reference ammonium carbamate.

Next to ammonium carbamate, white strings of another volatile were detected. Its FTIR spectrum (Fig. 7, Spectrum c) is identical to that of urea [29].

Other four volatile products condensed at the wall of the flask just above the foamed char, forming distinguishing rings. The top one formed white crystals and was identified as melamine (Fig. 7, Spectrum d) by comparison with the FTIR spectrum of a reference product. The less volatile product, the next ring lower, was of white color. Its FTIR spectrum (Spectrum e) exhibits the absorption bands of a phosphate ion (1229, 1089, 1048 cm^{-1}) and of a condensed melamine salt (1636 cm^{-1}). The presence of the symm-triazine ring of melamine is supported by its deformation vibration at 815 and 767 cm^{-1}.

The next two less volatile products were of gray color. Their FTIR spectra are indicative of melamine condensates (1630, 1555, 1460, 1401, 757 cm^{-1}) as well as of a condensed phosphate (1254, 1088, 982 cm^{-1}, Spectrum f) [24], and of a phosphate or monobasic phosphate (1232, 1086, 1046 cm^{-1}, Spectrum g). Carbonyl structures are detectable by the absorption band at 1736–1738 cm^{-1} (hydrolysis of melamine).

It is unlikely that melamine condensates volatilize on the pyrolysis of PEPAMP. They are likely to results from a vapor-phase reaction of evolved melamine and phosphoric acid.

The FTIR study did not reveal a formation of either PEPA-related HBPs or reaction products between PEPA and MP from the pyrolysis of PEPAMP.

3.5. *TOF MS study of PEPAMP*

In this study, a small quantity of PEPAMP was loaded onto the probe and directly inserted into the ion source. The temperature of the probe tip was rapidly heated to 600 °C, i.e. PEPAMP was subjected to a vacuum pyrolysis. Fig. 8 illustrates a typical TOF total ion chromatogram of volatile pyrolysis products. It is indicative of two main products, mass spectra of which are presented in Table 2, which also shows the assignment of the mass spectral peaks. The light one is a salt of a protonated PEPA and melamine, mass spectral

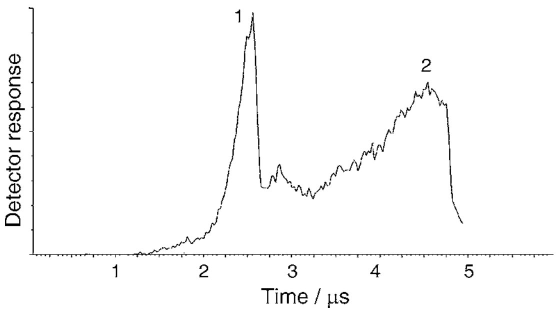

Fig. 8. TOF chromatogram of vacuum pyrolysis products of PEPAMP. Mass spectra of the products presented in Table 2.

Table 2
MS data of two vacuum pyrolysis products of PEPAMP

Abundance (%)	Ion (Da)		Formula	Assigned structure
	Experimental	Calculated		
Peak 1 in Fig. 7				
40	126.0651	126.0654	$C_3H_6N_6$	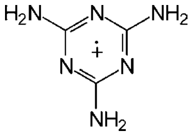
49	181.0268	181.0266	$C_5H_{10}O_5P$	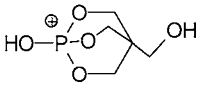
10	253.1386	253.1386	$C_6H_{13}N_{12}$	Protonated dimer of melamine
100	307.0890	307.0920	$C_8H_{16}N_6O_5P$	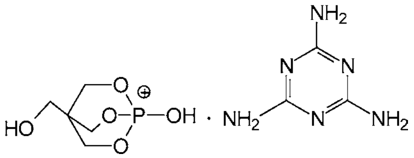
Peak 2 in Fig. 7				
30	98.9845	98.9845	H_4O_4P	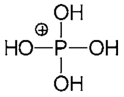
100	127.0739	127.073912	$C_3H_7N_6$	Protonated melamine
22	196.9633	196.9616	$H_7O_8P_2$	Protonated dimer of phosphoric acid
6	225.0479	225.0501	$C_3H_{10}N_6O_4P$	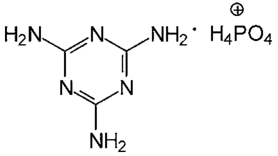
10	351.1116	351.1155	$C_6H_{16}N_{12}O_4P$	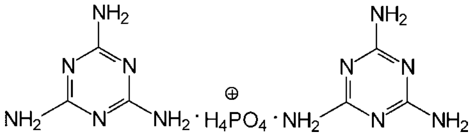

fragmentation of which is accompanied by formation of the protonated PEPA and melamine.

The heavy product (Table 2) is a protonated dimelamine phosphate. It shows successive losses of melamine to form the protonated phosphoric acid. Alternatively, melamine phosphate can be eliminated yielding the protonated melamine.

In conclusion, the vacuum pyrolysis of PEPAMP reveals the formation of a reaction product of PEPA and melamine, and dimelamine phosphate being the primary pyrolysis products. The formation of dimelamine phosphate is in agreement with the FTIR study of volatile products where condensation and hydrolysis products of melamine phosphate were found, being the secondary pyrolysis products. The reaction product of PEPA and melamine is likely to undergo further condensed state decomposition under the nitrogen flow pyrolysis and therefore was not observed among the HBPs.

3.6. Thermal decomposition of PEPAMP

After melting of PEPA at 218 °C, dehydration of MP starts to form melamine pyrophosphate followed by reaction with PEPA. One of possible reactions can be reaction of the pyrophosphate linkage P–O–P with the alcoholic group of PEPA, as shown in Fig. 5B. In this way, the HO– group will be destroyed (Fig. 6, Spectrum b), yielding a phosphorylated PEPA. However, the PEPA bicycle will remain intact in the course of this reaction.

As shown by the DSC and FTIR data, melamine exhibits a destructive effect on PEPA. Primary aromatic amines are reported [30] to be alkylated with trialkyl phosphates. Melamine is known [31] to react with dialkyl phosphonates or trialkyl phosphates at 100 °C, producing monoalkylmelaminium phosphonate or phosphate and/or melaminium phosphonate or phosphate. In a similar way, alkylation of melamine is likely to occur from a mixture of PEPA and MP followed by the formation of alkylated melamine salt. A reaction product of PEPA and MP has been supported by the TOF MS study, and its further rearrangement to an alkylated melamine cannot be excluded.

In the next step above 250 °C, phosphates of the condensates of melamine are produced with evolution of ammonia, which together with evolved water causes foaming of the

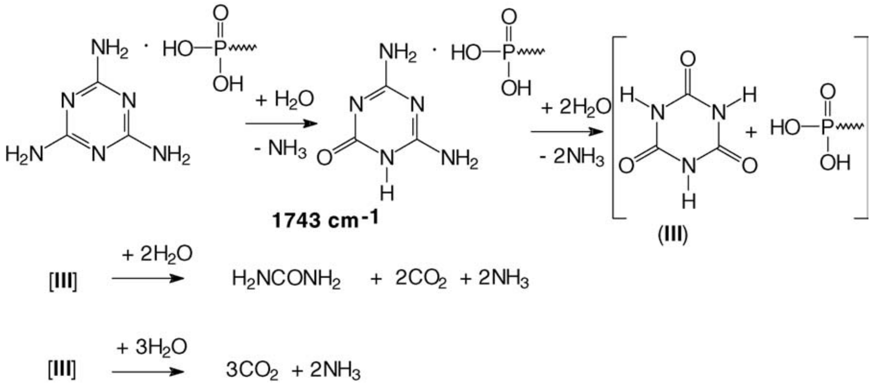

Fig. 9. Proposed mechanism of the low-temperature decomposition of melamine phospate.

material. At this step of the thermal decomposition, formation of carbonyl compounds also occurs, most likely due to hydrolysis of melamine [32]. A proposed mechanism shown in Fig. 9 is supported by the formation of urea and ammonium carbamate in the HBPs. According to this mechanism, a successive hydrolysis of melamine takes place to form carbon dioxide, ammonia or urea. In the gas-phase, reaction of carbon dioxide and ammonia leads to the formation of ammonium carbamate (Fig. 7, Spectrum b). However, the hydrolysis reaction is not a dominant one, as CO_2 is a minor gaseous product, whereas ammonia is a major one. The main source of ammonia is the condensation reaction of melamine.

Melamine phosphate shows loss of the melamine structure with formation of free –C≡N groups, starting from 650 °C [13]. In the present study, a first sign of loss of the melamine ring is observed at 300 °C (Fig. 6c), indicating its low-temperature decomposition. A similar effect was reported from pyrolysis of HIPS fire retarded with a mixture of melamine and a derivative of a phosphinic acid at 300 °C, where the formation of carbon dioxide and urea derivatives was found [33], and from pyrolysis of HIPS fire retarded with melamine polyphosphate [34]. Pure melamine phosphate does not show this reaction [13].

Before 400 °C (Fig. 6d) liberation of polyphosphoric acids takes place, which causes the charring of the material. The acids are a substantial part of condensed-phase flame retardancy as their coating acts as a physical barrier to the vaporization of fuel (combustible gaseous products emitted during thermal decomposition of polymeric materials) and can deactivate oxidation-active centres on the carbon [35].

Formation of P–N-containing products, phosphoramidates, is not evident from this study. Indirect evidence might be the appearance of ammonium in the sample pyrolyzed at 500 °C (Fig. 6, spectrum e). It cannot survive temperature of 500 °C, however can result from hydrolysis of imidophosphoric acids formed during thermal decomposition of PEPAMP.

4. Conclusions

PEPA is a thermally stable to 220 °C compound, a foamed char yield from which exceeds 45%. However, PEPA decomposes exothermally and this can negate the thermal insulating characteristic of the char and additionally warm up the bulk of the polymer. In respect with this, the addition of MP to PEPA shows a positive outcome, as the exothermal effects are essentially lowered. Both PEPA and PEPAMP produce equal amount of char, however, that of PEPAMP is less stable to the oxidative degradation.

The condensed-phase chemistry of the char formation of PEPAMP involves reaction between PEPA and melamine, formation of melamine condensates and polyphosphoric acids, and a low-temperature decomposition of melamine, yielding carbon dioxide and ammonia.

Acknowledgment

The author is grateful to Mr. G. Zwick for a number of helpful discussions of the TOF MS analysis.

References

[1] G. Camino, R. Delobel, in: A.F. Grand, Ch.A. Wilkie (Eds.), Fire Retardancy of Polymeric Materials, Marcel Dekker, New York, 2000, pp. 217–243.
[2] H.L. Vandersall, J. Fire Flamm. 2 (1971) 97–140.
[3] W.A. Hills, US Patent 3,873,496 (1975).
[4] Y. Tamura, R. Tanaka, US Patent 4,584,331 (1983).
[5] X. Li, Y. Ou, Y. Shi, Polym. Degr. Stab. 77 (2002) 383–390.
[6] E.J. Termine, N.A. Favstritsky, K.G. Taylor, US Patent 5,346,938 (1991).
[7] A.I. Balabanovich, G.F. Levchik, F. Gruber, Proceedings of the IV International Scientific Conference "Polymer Composites, Coatings, Films", Gomel, Belarus, July 22–24, 2003, pp. 186–187.
[8] Y. Halpern, US Patent 4,341,694 (1982).
[9] W.J. Parr, A.G. Mack, P.Y.Y. Moy, US Patent 4,801,625 (1987).
[10] G. Camino, G. Martinasso, L. Costa, Polym. Degr. Stab. 27 (1990) 285–296.

[11] G. Camino, G. Martinasso, L. Costa, R. Gobetto, Polym. Degr. Stab. 28 (1990) 17–38.

[12] E. Weil, B. McSwigan, J. Coatings Technol. 66 (1994) 75–82.

[13] L. Costa, G. Camino, M.P. Luda di Cortemiglia, Fire and polymers, in: G. Nelson (Ed.), ACS Symposium Ser., vol. 425, ACS, Washington, DC, 1990, pp. 211–238.

[14] S.I. Volfkovič, W. Feldmann, M.L. Kozmina, Z. Anorg. Allg. Chem. 457 (1979) 20–30.

[15] R. Rätz, O.J. Sweeting, J. Org. Chem. 28 (1963) 1608–1612.

[16] G. Kamai, E.T. Mukmenev, Zhurnal Obshchei Khimii 33 (1963) 3197–3201 (in Russian).

[17] R.R. Shagidullin, N.A. Chadaeva, N.I. Zarubina, G.Kh. Kamai, Izvestia AN SSSR, Ser. Khimia (1966) 1543–1546 (in Russian).

[18] J. Hildbrand, G. Kaufmann, Spectrochim. Acta 26A (1970) 1407–1422.

[19] J. Hildbrand, G. Kaufmann, Bull. Soc. Chim. Fr. (1970) 876–881.

[20] L.C. Thomas, Interpretation of the Infrared Spectra of Organophosphorus Compounds, Heyden, London, 1974.

[21] N.B. Colthup, L.H. Daly, S.E. Wiberley, Introduction to Infrared and Raman Spectroscopy, third ed., Academic Press, Inc., London, 1990.

[22] K.D. Berlin, T.H. Austin, J. Org. Chem. 30 (1965) 2745–2748.

[23] A.E. Canavan, B.F. Dowden, C. Eaborn, J. Chem. Soc. (1962) 331–334.

[24] D.E.C. Corbridge, in: M. Grayson, E.J. Griffith (Eds.), Topics in Phosphorus Chemistry, vol. 6, Interscience, New York, 1969, pp. 251–365.

[25] D.O. Hummel, A. Solti, Atlas of Polymer and Plastics Analysis, vol. 2, part b/I, second ed., Carl Hanser Verlag, Munich, 1988.

[26] http://webbook.nist.gov/chemistry.

[27] A.I. Balabanovich, A.M. Balabanovich, J. Engelmann, Polym. Int. 52 (2003) 1309–1314.

[28] E.D. Weil, W. Zhu, N. Patel, S.M. Mukhopadhyay, Polym. Degr. Stab. 54 (1996) 125–136.

[29] A.Kh. Kuptsov, G.N. Zhizhin, Handbook of Fourier Transform Raman and Infrared Spectra of Polymers, Physmatlit, Moscow, 2001 (in Russian).

[30] T.L. Fletcher, M.E. Taylor, A.W. Dahl, J. Org. Chem. 20 (1955) 121–125.

[31] K. Troev, R. Tsevi, Phosphorus Sulfur Silicon 133 (1998) 61–68.

[32] E. Ichikara, T. Takizawa, K. Odo, J. Synth. Org. Chem. Jpn. 32 (1974) 936–939.

[33] A.I. Balabanovich, J. Fire Sci. 22 (2004) 163–178.

[34] U. Braun, B. Schartel, J. Fire Sci. 23 (2005) 5–29.

[35] M. Lewin, E.D. Weil, in: A.R. Horroks, D. Price (Eds.), Fire Retardant Materials, Woodhead Publishing Ltd., Cambridge, 2001, pp. 31–68.